

# The Scale Dependence of the Hadron Multiplicity in Quark and Gluon Jets and a Precise Determination of $C_A/C_F$

DELPHI Collaboration

## Abstract

Data collected at the Z resonance using the DELPHI detector at LEP are used to determine the charged hadron multiplicity in gluon and quark jets as a function of a transverse momentum-like scale. The colour factor ratio,  $C_A/C_F$ , is directly observed in the increase of multiplicities with that scale. The smaller than expected multiplicity ratio in gluon to quark jets is understood by differences in the hadronization of the leading quark or gluon. From the dependence of the charged hadron multiplicity on the opening angle in symmetric three-jet events the colour factor ratio is measured to be:

$$\frac{C_A}{C_F} = 2.246 \pm 0.062 \text{ (stat.)} \pm 0.080 \text{ (syst.)} \pm 0.095 \text{ (theo.)}$$

(Submitted to Physics Letters B)

P.Abreu<sup>21</sup>, W.Adam<sup>50</sup>, T.Adye<sup>36</sup>, P.Adzic<sup>11</sup>, I.Ajinenko<sup>42</sup>, Z.Albrecht<sup>17</sup>, T.Alderweireld<sup>2</sup>, G.D.Alekseev<sup>16</sup>, R.Aleman<sup>49</sup>, T.Allmendinger<sup>17</sup>, P.P.Allport<sup>22</sup>, S.Almehed<sup>24</sup>, U.Amaldi<sup>9</sup>, S.Amato<sup>47</sup>, E.G.Anassontzis<sup>3</sup>, P.Andersson<sup>44</sup>, A.Andreazza<sup>9</sup>, S.Andringa<sup>21</sup>, P.Antilogus<sup>25</sup>, W-D.Apel<sup>17</sup>, Y.Arnoud<sup>9</sup>, B.Åsman<sup>44</sup>, J-E.Augustin<sup>25</sup>, A.Augustinus<sup>9</sup>, P.Baillon<sup>9</sup>, P.Bambade<sup>19</sup>, F.Barao<sup>21</sup>, G.Barbiellini<sup>46</sup>, R.Barbier<sup>25</sup>, D.Y.Bardin<sup>16</sup>, G.Barker<sup>9</sup>, A.Baroncelli<sup>38</sup>, M.Battaglia<sup>15</sup>, M.Baumbach<sup>23</sup>, K-H.Becks<sup>52</sup>, M.Begalli<sup>6</sup>, P.Beilliere<sup>8</sup>, Yu.Belokopytov<sup>9,53</sup>, A.C.Benvenuti<sup>5</sup>, C.Berat<sup>14</sup>, M.Berggren<sup>25</sup>, D.Bertini<sup>25</sup>, D.Bertrand<sup>2</sup>, M.Besancon<sup>39</sup>, F.Bianchi<sup>45</sup>, M.Bigi<sup>45</sup>, M.S.Bilenky<sup>16</sup>, M-A.Bizouard<sup>19</sup>, D.Bloch<sup>10</sup>, H.M.Blom<sup>30</sup>, M.Bonesini<sup>27</sup>, W.Bonivento<sup>27</sup>, M.Boonekamp<sup>39</sup>, P.S.L.Booth<sup>22</sup>, A.W.Borgland<sup>4</sup>, G.Borisov<sup>19</sup>, C.Bosio<sup>41</sup>, O.Botner<sup>48</sup>, E.Boudinov<sup>30</sup>, B.Bouquet<sup>19</sup>, C.Bourdarios<sup>19</sup>, T.J.V.Bowcock<sup>22</sup>, I.Boyko<sup>16</sup>, I.Bozovic<sup>11</sup>, M.Bozzo<sup>13</sup>, P.Branchini<sup>38</sup>, T.Brenke<sup>52</sup>, R.A.Brenner<sup>48</sup>, P.Bruckman<sup>18</sup>, J-M.Brunet<sup>8</sup>, L.Bugge<sup>32</sup>, T.Buran<sup>32</sup>, T.Burgsmueller<sup>52</sup>, P.Buschmann<sup>52</sup>, S.Cabrera<sup>49</sup>, M.Caccia<sup>27</sup>, M.Calvi<sup>27</sup>, A.J.Camacho Rozas<sup>40</sup>, T.Camporesi<sup>9</sup>, V.Canale<sup>37</sup>, F.Carena<sup>9</sup>, L.Carroll<sup>22</sup>, C.Caso<sup>13</sup>, M.V.Castillo Gimenez<sup>49</sup>, A.Cattai<sup>9</sup>, F.R.Cavallo<sup>5</sup>, V.Chabaud<sup>9</sup>, Ph.Charpentier<sup>9</sup>, L.Chaussard<sup>25</sup>, P.Checchia<sup>35</sup>, G.A.Chelkov<sup>16</sup>, R.Chierici<sup>45</sup>, P.Chliapnikov<sup>42</sup>, P.Chochula<sup>7</sup>, V.Chorowicz<sup>25</sup>, J.Chudoba<sup>29</sup>, P.Collins<sup>9</sup>, R.Contri<sup>13</sup>, E.Cortina<sup>49</sup>, G.Cosme<sup>19</sup>, F.Cossutti<sup>9</sup>, J-H.Cowell<sup>22</sup>, H.B.Crawley<sup>1</sup>, D.Crennell<sup>36</sup>, S.Crepe<sup>14</sup>, G.Crosetti<sup>13</sup>, J.Cuevas Maestro<sup>33</sup>, S.Czellar<sup>15</sup>, G.Damgaard<sup>28</sup>, M.Davenport<sup>9</sup>, W.Da Silva<sup>23</sup>, A.Deghorain<sup>2</sup>, G.Della Ricca<sup>46</sup>, P.Delpierre<sup>26</sup>, N.Demaria<sup>9</sup>, A.De Angelis<sup>9</sup>, W.De Boer<sup>17</sup>, S.De Brabandere<sup>2</sup>, C.De Clercq<sup>2</sup>, B.De Lotto<sup>46</sup>, A.De Min<sup>35</sup>, L.De Paula<sup>47</sup>, H.Dijkstra<sup>9</sup>, L.Di Ciaccio<sup>37</sup>, J.Dolbeau<sup>8</sup>, K.Doroba<sup>51</sup>, M.Dracos<sup>10</sup>, J.Drees<sup>52</sup>, M.Dris<sup>31</sup>, A.Duperrin<sup>25</sup>, J-D.Durand<sup>9</sup>, G.Eigen<sup>4</sup>, T.Ekelof<sup>48</sup>, G.Ekspong<sup>44</sup>, M.Ellert<sup>48</sup>, M.Elsing<sup>9</sup>, J-P.Engel<sup>10</sup>, B.Erzen<sup>43</sup>, M.Espirito Santo<sup>21</sup>, E.Falk<sup>24</sup>, G.Fanourakis<sup>11</sup>, D.Fassouliotis<sup>11</sup>, J.Fayot<sup>23</sup>, M.Feindt<sup>17</sup>, P.Ferrari<sup>27</sup>, A.Ferrer<sup>49</sup>, E.Ferrer-Ribas<sup>19</sup>, S.Fichet<sup>23</sup>, A.Firestone<sup>1</sup>, U.Flagmeyer<sup>52</sup>, H.Foeth<sup>9</sup>, E.Fokitis<sup>31</sup>, F.Fontanelli<sup>13</sup>, B.Franek<sup>36</sup>, A.G.Frodesen<sup>4</sup>, R.Fruhworth<sup>50</sup>, F.Fulda-Quenzer<sup>19</sup>, J.Fuster<sup>49</sup>, A.Galloni<sup>22</sup>, D.Gamba<sup>45</sup>, S.Gamblin<sup>19</sup>, M.Gandelman<sup>47</sup>, C.Garcia<sup>49</sup>, J.Garcia<sup>40</sup>, C.Gaspar<sup>9</sup>, M.Gaspar<sup>47</sup>, U.Gasparini<sup>35</sup>, Ph.Gavillet<sup>9</sup>, E.N.Gazis<sup>31</sup>, D.Gele<sup>10</sup>, L.Gerdyukov<sup>42</sup>, N.Ghodbane<sup>25</sup>, I.Gil<sup>49</sup>, F.Glege<sup>52</sup>, R.Gokieli<sup>9,51</sup>, B.Golob<sup>43</sup>, G.Gomez-Ceballos<sup>40</sup>, P.Goncalves<sup>21</sup>, I.Gonzalez Caballero<sup>40</sup>, G.Gopal<sup>36</sup>, L.Gorn<sup>1,54</sup>, M.Gorski<sup>51</sup>, Yu.Gou<sup>42</sup>, V.Gracco<sup>13</sup>, J.Grahl<sup>1</sup>, E.Graziani<sup>38</sup>, C.Green<sup>22</sup>, H-J.Grimm<sup>17</sup>, P.Gris<sup>39</sup>, G.Grosdidier<sup>19</sup>, K.Grzelak<sup>51</sup>, M.Gunther<sup>48</sup>, J.Guy<sup>36</sup>, F.Hahn<sup>9</sup>, S.Hahn<sup>52</sup>, S.Haider<sup>9</sup>, A.Hallgren<sup>48</sup>, K.Hamacher<sup>52</sup>, J.Hansen<sup>32</sup>, F.J.Harris<sup>34</sup>, V.Hedberg<sup>24</sup>, S.Heising<sup>17</sup>, J.J.Hernandez<sup>49</sup>, P.Herquet<sup>2</sup>, H.Herr<sup>9</sup>, T.L.Hessing<sup>34</sup>, J.-M.Heuser<sup>52</sup>, E.Higon<sup>49</sup>, S-O.Holmgren<sup>44</sup>, P.J.Holt<sup>34</sup>, S.Hoorelbeke<sup>2</sup>, M.Houlden<sup>22</sup>, J.Hrubic<sup>50</sup>, K.Huet<sup>2</sup>, G.J.Hughes<sup>22</sup>, K.Hultqvist<sup>44</sup>, J.N.Jackson<sup>22</sup>, R.Jacobsson<sup>9</sup>, P.Jalocha<sup>9</sup>, R.Janik<sup>7</sup>, Ch.Jarlskog<sup>24</sup>, G.Jarlskog<sup>24</sup>, P.Jarry<sup>39</sup>, B.Jean-Marie<sup>19</sup>, E.K.Johansson<sup>44</sup>, P.Jonsson<sup>25</sup>, C.Joram<sup>9</sup>, P.Juillot<sup>10</sup>, F.Kapusta<sup>23</sup>, K.Karafasoulis<sup>11</sup>, S.Katsanevas<sup>25</sup>, E.C.Katsoufis<sup>31</sup>, R.Keranen<sup>17</sup>, B.P.Kersevan<sup>43</sup>, B.A.Khomenko<sup>16</sup>, N.N.Khovanski<sup>16</sup>, A.Kiiskinen<sup>15</sup>, B.King<sup>22</sup>, A.Kinwig<sup>22</sup>, N.J.Kjaer<sup>30</sup>, O.Klapp<sup>52</sup>, H.Klein<sup>9</sup>, P.Kluit<sup>30</sup>, P.Kokkinias<sup>11</sup>, M.Koratzinos<sup>9</sup>, V.Kostioukhine<sup>42</sup>, C.Kourkoumelis<sup>3</sup>, O.Kouznetsov<sup>16</sup>, M.Krammer<sup>50</sup>, E.Kriznic<sup>43</sup>, J.Krstic<sup>11</sup>, Z.Krumstein<sup>16</sup>, P.Kubinec<sup>7</sup>, W.Kucewicz<sup>18</sup>, J.Kurowska<sup>51</sup>, K.Kurvinen<sup>15</sup>, J.W.Lamsa<sup>1</sup>, D.W.Lane<sup>1</sup>, P.Langefeld<sup>52</sup>, V.Lapin<sup>42</sup>, J-P.Laugier<sup>39</sup>, R.Lauhakangas<sup>15</sup>, G.Leder<sup>50</sup>, F.Ledroit<sup>14</sup>, V.Lefebure<sup>2</sup>, L.Leinonen<sup>44</sup>, A.Leisos<sup>11</sup>, R.Leitner<sup>29</sup>, J.Lemonne<sup>2</sup>, G.Lenzen<sup>52</sup>, V.Lepeltier<sup>19</sup>, T.Lesiak<sup>18</sup>, M.Lethuillier<sup>39</sup>, J.Libby<sup>34</sup>, D.Liko<sup>9</sup>, A.Lipniacka<sup>44</sup>, I.Lippi<sup>35</sup>, B.Loerstad<sup>24</sup>, J.G.Loken<sup>34</sup>, J.H.Lopes<sup>47</sup>, J.M.Lopez<sup>40</sup>, R.Lopez-Fernandez<sup>14</sup>, D.Loukas<sup>11</sup>, P.Lutz<sup>39</sup>, L.Lyons<sup>34</sup>, J.MacNaughton<sup>50</sup>, J.R.Mahon<sup>6</sup>, A.Maio<sup>21</sup>, A.Malek<sup>52</sup>, T.G.M.Malmgren<sup>44</sup>, V.Malychev<sup>16</sup>, F.Mandi<sup>50</sup>, J.Marco<sup>40</sup>, R.Marco<sup>40</sup>, B.Marechal<sup>47</sup>, M.Margoni<sup>35</sup>, J-C.Marin<sup>9</sup>, C.Mariotti<sup>9</sup>, A.Markou<sup>11</sup>, C.Martinez-Rivero<sup>19</sup>, F.Martinez-Vidal<sup>49</sup>, S.Marti i Garcia<sup>9</sup>, J.Masik<sup>12</sup>, N.Mastroiannopoulos<sup>11</sup>, F.Matorras<sup>40</sup>, C.Matteuzzi<sup>27</sup>, G.Matthiae<sup>37</sup>, F.Mazzucato<sup>35</sup>, M.Mazzucato<sup>35</sup>, M.Mc Cubbin<sup>22</sup>, R.Mc Kay<sup>1</sup>, R.Mc Nulty<sup>22</sup>, G.Mc Pherson<sup>22</sup>, C.Meroni<sup>27</sup>, W.T.Meyer<sup>1</sup>, A.Miagkov<sup>42</sup>, E.Migliore<sup>45</sup>, L.Mirabito<sup>25</sup>, W.A.Mitaroff<sup>50</sup>, U.Mjoernmark<sup>24</sup>, T.Moa<sup>44</sup>, M.Moch<sup>17</sup>, R.Moeller<sup>28</sup>, K.Moenig<sup>9</sup>, M.R.Monge<sup>13</sup>, X.Moreau<sup>23</sup>, P.Morettini<sup>13</sup>, G.Morton<sup>34</sup>, U.Mueller<sup>52</sup>, K.Muenich<sup>52</sup>, M.Mulders<sup>30</sup>, C.Mulet-Marquis<sup>14</sup>, R.Muresan<sup>24</sup>, W.J.Murray<sup>36</sup>, B.Muryn<sup>14,18</sup>, G.Myatt<sup>34</sup>, T.Myklebust<sup>32</sup>, F.Naraghi<sup>14</sup>, F.L.Navarria<sup>5</sup>, S.Navas<sup>49</sup>, K.Nawrocki<sup>51</sup>, P.Negri<sup>27</sup>, S.Nemecek<sup>12</sup>, N.Neufeld<sup>9</sup>, N.Neumeister<sup>50</sup>, R.Nicolaidou<sup>14</sup>, B.S.Nielsen<sup>28</sup>, M.Nikolenko<sup>10,16</sup>, V.Nomokonov<sup>15</sup>, A.Normand<sup>22</sup>, A.Nygren<sup>24</sup>, V.Obraztsov<sup>42</sup>, A.G.Olshevski<sup>16</sup>, A.Onofre<sup>21</sup>, R.Orava<sup>15</sup>, G.Orazi<sup>10</sup>, K.Osterberg<sup>15</sup>, A.Ouraou<sup>39</sup>, M.Paganoni<sup>27</sup>, S.Paiano<sup>5</sup>, R.Pain<sup>23</sup>, R.Paiva<sup>21</sup>, J.Palacios<sup>34</sup>, H.Palka<sup>18</sup>, Th.D.Papadopoulou<sup>31</sup>, K.Papageorgiou<sup>11</sup>, L.Pape<sup>9</sup>, C.Parkes<sup>9</sup>, F.Parodi<sup>13</sup>, U.Parzefall<sup>22</sup>, A.Passerì<sup>38</sup>, O.Passon<sup>52</sup>, M.Pegoraro<sup>35</sup>, L.Peralta<sup>21</sup>, A.Perrotta<sup>5</sup>, C.Petridou<sup>46</sup>, A.Petrolini<sup>13</sup>, H.T.Phillips<sup>36</sup>, F.Pierre<sup>39</sup>, M.Pimenta<sup>21</sup>, E.Piotto<sup>27</sup>, T.Podobnik<sup>43</sup>, M.E.Pol<sup>6</sup>, G.Polok<sup>18</sup>, P.Poropat<sup>46</sup>, V.Pozdniakov<sup>16</sup>, P.Privitera<sup>37</sup>, N.Pukhaeva<sup>16</sup>, A.Pullia<sup>27</sup>, D.Radojicic<sup>34</sup>, S.Ragazzi<sup>27</sup>, H.Rahmani<sup>31</sup>, D.Rakoczy<sup>50</sup>, P.N.Ratoff<sup>20</sup>, A.L.Read<sup>32</sup>, P.Rebecchi<sup>9</sup>, N.G.Redaeli<sup>27</sup>, M.Regler<sup>50</sup>, D.Reid<sup>30</sup>, R.Reinhardt<sup>52</sup>, P.B.Renton<sup>34</sup>, L.K.Resvanis<sup>3</sup>, F.Richard<sup>19</sup>, J.Ridky<sup>12</sup>, G.Rinaudo<sup>45</sup>, O.Rohne<sup>32</sup>, A.Romero<sup>45</sup>, P.Ronchese<sup>35</sup>, E.I.Rosenberg<sup>1</sup>, P.Rosinsky<sup>7</sup>, P.Roudeau<sup>19</sup>, T.Rovelli<sup>5</sup>, Ch.Royon<sup>39</sup>, V.Ruhmann-Kleider<sup>39</sup>, A.Ruiz<sup>40</sup>, H.Saarikko<sup>15</sup>, Y.Sacquin<sup>39</sup>, A.Sadovsky<sup>16</sup>, G.Sajot<sup>14</sup>, J.Salt<sup>49</sup>, D.Sampsonidis<sup>11</sup>, M.Sannino<sup>13</sup>, H.Schneider<sup>17</sup>, Ph.Schwemling<sup>23</sup>, U.Schwickerath<sup>17</sup>, M.A.E.Schyns<sup>52</sup>, F.Scuri<sup>46</sup>, P.Seager<sup>20</sup>, Y.Sedykh<sup>16</sup>, A.M.Segar<sup>34</sup>, R.Sekulin<sup>36</sup>, R.C.Shellard<sup>6</sup>, A.Sheridan<sup>22</sup>, M.Siebel<sup>52</sup>, L.Simard<sup>39</sup>, F.Simonetto<sup>35</sup>, A.N.Sisakian<sup>16</sup>, G.Smadja<sup>25</sup>, O.Smirnova<sup>24</sup>, G.R.Smith<sup>36</sup>, A.Sokolov<sup>42</sup>, O.Solovianov<sup>42</sup>, A.Sopczak<sup>17</sup>, R.Sosnowski<sup>51</sup>, T.Spassov<sup>21</sup>, E.Spiriti<sup>38</sup>, P.Sponholz<sup>52</sup>, S.Squarcia<sup>13</sup>, D.Stamper<sup>50</sup>, C.Stanescu<sup>38</sup>, S.Stanic<sup>43</sup>, K.Stevenson<sup>34</sup>, A.Stocchi<sup>19</sup>, J.Strauss<sup>50</sup>, R.Strub<sup>10</sup>, B.Stugu<sup>4</sup>, M.Szczekowski<sup>51</sup>, M.Szeptycka<sup>51</sup>, T.Tabarelli<sup>27</sup>, F.Tegenfeldt<sup>48</sup>, F.Terranova<sup>27</sup>, J.Thomas<sup>34</sup>, J.Timmermans<sup>30</sup>, N.Tinti<sup>5</sup>,

L.G.Tkatchev<sup>16</sup>, S.Todorova<sup>10</sup>, B.Tome<sup>21</sup>, A.Tonazzo<sup>9</sup>, L.Tortora<sup>38</sup>, G.Transtrome<sup>24</sup>, D.Treille<sup>9</sup>, G.Tristram<sup>8</sup>, M.Trochimczuk<sup>51</sup>, C.Troncon<sup>27</sup>, A.Tsirou<sup>9</sup>, M-L.Turluer<sup>39</sup>, I.A.Tyapkin<sup>16</sup>, S.Tzamarias<sup>11</sup>, B.Ueberschaer<sup>52</sup>, O.Ullaland<sup>9</sup>, V.Uvarov<sup>42</sup>, G.Valenti<sup>5</sup>, E.Vallazza<sup>46</sup>, G.W.Van Apeldoorn<sup>30</sup>, P.Van Dam<sup>30</sup>, J.Van Eldik<sup>30</sup>, A.Van Lysebetten<sup>2</sup>, I.Van Vulpen<sup>30</sup>, N.Vassilopoulos<sup>34</sup>, G.Vegni<sup>27</sup>, L.Ventura<sup>35</sup>, W.Venus<sup>36,9</sup>, F.Verbeure<sup>2</sup>, M.Verlato<sup>35</sup>, L.S.Vertogradov<sup>16</sup>, V.Verzi<sup>37</sup>, D.Vilanova<sup>39</sup>, L.Vitale<sup>46</sup>, E.Vlasov<sup>42</sup>, A.S.Vodopyanov<sup>16</sup>, C.Vollmer<sup>17</sup>, G.Voulgaris<sup>3</sup>, V.Vrba<sup>12</sup>, H.Wahlen<sup>52</sup>, C.Walck<sup>44</sup>, C.Weiser<sup>17</sup>, D.Wicke<sup>52</sup>, J.H.Wickens<sup>2</sup>, G.R.Wilkinson<sup>9</sup>, M.Winter<sup>10</sup>, M.Witek<sup>18</sup>, G.Wolf<sup>9</sup>, J.Yi<sup>1</sup>, O.Yushchenko<sup>42</sup>, A.Zalewska<sup>18</sup>, P.Zalewski<sup>51</sup>, D.Zavrtanik<sup>43</sup>, E.Zevgolatakos<sup>11</sup>, N.I.Zimin<sup>16,24</sup>, G.C.Zucchelli<sup>44</sup>, G.Zumerle<sup>35</sup>

<sup>1</sup>Department of Physics and Astronomy, Iowa State University, Ames IA 50011-3160, USA

<sup>2</sup>Physics Department, Univ. Instelling Antwerpen, Universiteitsplein 1, BE-2610 Wilrijk, Belgium and IIHE, ULB-VUB, Pleinlaan 2, BE-1050 Brussels, Belgium

and Faculté des Sciences, Univ. de l'Etat Mons, Av. Maistriau 19, BE-7000 Mons, Belgium

<sup>3</sup>Physics Laboratory, University of Athens, Solonos Str. 104, GR-10680 Athens, Greece

<sup>4</sup>Department of Physics, University of Bergen, Allégaten 55, NO-5007 Bergen, Norway

<sup>5</sup>Dipartimento di Fisica, Università di Bologna and INFN, Via Irnerio 46, IT-40126 Bologna, Italy

<sup>6</sup>Centro Brasileiro de Pesquisas Físicas, rua Xavier Sigaud 150, BR-22290 Rio de Janeiro, Brazil

and Depto. de Física, Pont. Univ. Católica, C.P. 38071 BR-22453 Rio de Janeiro, Brazil

and Inst. de Física, Univ. Estadual do Rio de Janeiro, rua São Francisco Xavier 524, Rio de Janeiro, Brazil

<sup>7</sup>Comenius University, Faculty of Mathematics and Physics, Mlynska Dolina, SK-84215 Bratislava, Slovakia

<sup>8</sup>Collège de France, Lab. de Physique Corpusculaire, IN2P3-CNRS, FR-75231 Paris Cedex 05, France

<sup>9</sup>CERN, CH-1211 Geneva 23, Switzerland

<sup>10</sup>Institut de Recherches Subatomiques, IN2P3 - CNRS/ULP - BP20, FR-67037 Strasbourg Cedex, France

<sup>11</sup>Institute of Nuclear Physics, N.C.S.R. Demokritos, P.O. Box 60228, GR-15310 Athens, Greece

<sup>12</sup>FZU, Inst. of Phys. of the C.A.S. High Energy Physics Division, Na Slovance 2, CZ-180 40, Praha 8, Czech Republic

<sup>13</sup>Dipartimento di Fisica, Università di Genova and INFN, Via Dodecaneso 33, IT-16146 Genova, Italy

<sup>14</sup>Institut des Sciences Nucléaires, IN2P3-CNRS, Université de Grenoble 1, FR-38026 Grenoble Cedex, France

<sup>15</sup>Helsinki Institute of Physics, HIP, P.O. Box 9, FI-00014 Helsinki, Finland

<sup>16</sup>Joint Institute for Nuclear Research, Dubna, Head Post Office, P.O. Box 79, RU-101 000 Moscow, Russian Federation

<sup>17</sup>Institut für Experimentelle Kernphysik, Universität Karlsruhe, Postfach 6980, DE-76128 Karlsruhe, Germany

<sup>18</sup>Institute of Nuclear Physics and University of Mining and Metallurgy, Ul. Kawiora 26a, PL-30055 Krakow, Poland

<sup>19</sup>Université de Paris-Sud, Lab. de l'Accélérateur Linéaire, IN2P3-CNRS, Bât. 200, FR-91405 Orsay Cedex, France

<sup>20</sup>School of Physics and Chemistry, University of Lancaster, Lancaster LA1 4YB, UK

<sup>21</sup>LIP, IST, FCUL - Av. Elias Garcia, 14-1<sup>o</sup>, PT-1000 Lisboa Codex, Portugal

<sup>22</sup>Department of Physics, University of Liverpool, P.O. Box 147, Liverpool L69 3BX, UK

<sup>23</sup>LPNHE, IN2P3-CNRS, Univ. Paris VI et VII, Tour 33 (RdC), 4 place Jussieu, FR-75252 Paris Cedex 05, France

<sup>24</sup>Department of Physics, University of Lund, Sölvegatan 14, SE-223 63 Lund, Sweden

<sup>25</sup>Université Claude Bernard de Lyon, IPNL, IN2P3-CNRS, FR-69622 Villeurbanne Cedex, France

<sup>26</sup>Univ. d'Aix - Marseille II - CPP, IN2P3-CNRS, FR-13288 Marseille Cedex 09, France

<sup>27</sup>Dipartimento di Fisica, Università di Milano and INFN, Via Celoria 16, IT-20133 Milan, Italy

<sup>28</sup>Niels Bohr Institute, Blegdamsvej 17, DK-2100 Copenhagen Ø, Denmark

<sup>29</sup>NC, Nuclear Centre of MFF, Charles University, Areal MFF, V Holesovickach 2, CZ-180 00, Praha 8, Czech Republic

<sup>30</sup>NIKHEF, Postbus 41882, NL-1009 DB Amsterdam, The Netherlands

<sup>31</sup>National Technical University, Physics Department, Zografou Campus, GR-15773 Athens, Greece

<sup>32</sup>Physics Department, University of Oslo, Blindern, NO-1000 Oslo 3, Norway

<sup>33</sup>Dpto. Física, Univ. Oviedo, Avda. Calvo Sotelo s/n, ES-33007 Oviedo, Spain

<sup>34</sup>Department of Physics, University of Oxford, Keble Road, Oxford OX1 3RH, UK

<sup>35</sup>Dipartimento di Fisica, Università di Padova and INFN, Via Marzolo 8, IT-35131 Padua, Italy

<sup>36</sup>Rutherford Appleton Laboratory, Chilton, Didcot OX11 0QX, UK

<sup>37</sup>Dipartimento di Fisica, Università di Roma II and INFN, Tor Vergata, IT-00173 Rome, Italy

<sup>38</sup>Dipartimento di Fisica, Università di Roma III and INFN, Via della Vasca Navale 84, IT-00146 Rome, Italy

<sup>39</sup>DAPNIA/Service de Physique des Particules, CEA-Saclay, FR-91191 Gif-sur-Yvette Cedex, France

<sup>40</sup>Instituto de Física de Cantabria (CSIC-UC), Avda. los Castros s/n, ES-39006 Santander, Spain

<sup>41</sup>Dipartimento di Fisica, Università degli Studi di Roma La Sapienza, Piazzale Aldo Moro 2, IT-00185 Rome, Italy

<sup>42</sup>Inst. for High Energy Physics, Serpukov P.O. Box 35, Protvino, (Moscow Region), Russian Federation

<sup>43</sup>J. Stefan Institute, Jamova 39, SI-1000 Ljubljana, Slovenia and Laboratory for Astroparticle Physics, Nova Gorica Polytechnic, Kostanjevska 16a, SI-5000 Nova Gorica, Slovenia,

and Department of Physics, University of Ljubljana, SI-1000 Ljubljana, Slovenia

<sup>44</sup>Fysikum, Stockholm University, Box 6730, SE-113 85 Stockholm, Sweden

<sup>45</sup>Dipartimento di Fisica Sperimentale, Università di Torino and INFN, Via P. Giuria 1, IT-10125 Turin, Italy

<sup>46</sup>Dipartimento di Fisica, Università di Trieste and INFN, Via A. Valerio 2, IT-34127 Trieste, Italy

and Istituto di Fisica, Università di Udine, IT-33100 Udine, Italy

<sup>47</sup>Univ. Federal do Rio de Janeiro, C.P. 68528 Cidade Univ., Ilha do Fundão BR-21945-970 Rio de Janeiro, Brazil

<sup>48</sup>Department of Radiation Sciences, University of Uppsala, P.O. Box 535, SE-751 21 Uppsala, Sweden

<sup>49</sup>IFIC, Valencia-CSIC, and D.F.A.M.N., U. de Valencia, Avda. Dr. Moliner 50, ES-46100 Burjassot (Valencia), Spain

<sup>50</sup>Institut für Hochenergiephysik, Österr. Akad. d. Wissensch., Nikolsdorfergasse 18, AT-1050 Vienna, Austria

<sup>51</sup>Inst. Nuclear Studies and University of Warsaw, Ul. Hoza 69, PL-00681 Warsaw, Poland

<sup>52</sup>Fachbereich Physik, University of Wuppertal, Postfach 100 127, DE-42097 Wuppertal, Germany

<sup>53</sup>On leave of absence from IHEP Serpukhov

<sup>54</sup>Now at University of Florida

# 1 Introduction

The gauge symmetry underlying the Lagrangian of an interaction directly determines the relative coupling of the vertices of the participating elementary fields. A comparison of the properties of quark and gluon jets, which are linked to the quark and gluon couplings, therefore implies a direct and intuitive test of Quantum Chromodynamics, QCD, the gauge theory of the strong interaction.

Hadron production can be described via a so-called parton shower, a chain of successive bremsstrahlung processes, followed by hadron formation which cannot be described perturbatively. As bremsstrahlung is directly proportional to the coupling of the radiated vector boson to the radiator, the ratio of the radiated gluon multiplicity from a gluon and quark source is expected to be asymptotically equal to the ratio of the QCD colour factors:  $C_A/C_F = 9/4$  [1]. As the radiated gluons give rise to the production of hadrons, the increased radiation from gluons should be reflected in a higher hadron multiplicity and also in a stronger scaling violation of the gluon fragmentation function [2,3].

It was however noted already in the first paper comparing the multiplicities from gluons and quarks [1] that this prediction does not immediately apply to the observed charged hadron multiplicities at finite energy as this is also influenced by differences of the fragmentation of the primary quark or gluon. These differences must be present because quarks are valence particles of the hadrons whereas gluons are not. This is most clearly evident from the behaviour of the gluon fragmentation function to charged hadrons at large scaled momentum where it is suppressed by about one order of magnitude compared to the quark fragmentation function [3]. This suppression also causes a higher multiplicity to be expected from very low energy quark jets compared to gluon jets. Moreover, as low momentum, large wavelength gluons cannot resolve a hard radiated gluon from the initial quark-antiquark pair in the early phase of an event, soft radiation and correspondingly the production of low energy hadrons is further suppressed [4–6] compared to the naive expectation. In a previous publication [2] it has been shown that a reduction of the primary splittings of gluons compared to the perturbative expectation is indeed responsible for the observed small hadron multiplicity ratio between gluon and quark jets.

If heavy quark jets are also included in the comparison, a further reduction of the multiplicity ratio is evident due to the high number of particles from the decays of the primary heavy particles.

Furthermore, the definition of quark and gluon jets in three-jet events in  $e^+e^-$  annihilation uses jet algorithms which combine hadrons to make jets. Low energy particles at large angles with respect to the original parton direction are likely to be assigned to a different jet. As gluon jets are initially wider than quark jets this presumably leads to a loss of multiplicity for gluon jets and a corresponding gain for quark jets.

The effects discussed lead to a ratio between the charged hadron multiplicities from gluon and quark jets being smaller than the ratio between gluon radiation from gluons and from quarks. So far these effects have mainly been neglected in experimental and more elaborate theoretical investigations [7]. However, as we will show in this paper, at current energies these non-perturbative effects are still important and need to be considered in a proper test of the prediction [1] that the radiated gluon-to-quark multiplicity ratio is equal to the colour factor ratio.

The stronger radiation from gluons is expected to become directly evident from a stronger increase of the gluon jet multiplicity with the relevant energy scale as compared to quark jets. In this way the size of the non-perturbative terms can also be directly

estimated from the quark and gluon jet multiplicity at very small scales. A scale dependence of quark and gluon properties was first demonstrated in [8] with the jet energy as the intuitive scale. This result was later confirmed by other measurements [9–11] and has recently been extended to a transverse momentum-like scale [12].

A study of the *total* charged multiplicity of symmetric three-jet events as function of the internal scales of the event avoids some of the complications mentioned above. A novel precision measurement of the colour factor ratio  $C_A/C_F$  can be performed by combining these data with a Modified Leading Log Approximation (MLLA) prediction of the three-jet event multiplicity [13] which includes coherence of soft gluon radiation.

This letter is based on a data analysis which is similar to that presented in previous papers [2,8]. We therefore have restricted the experimental discussion in section 2 to the relevant differences with respect to these papers. More detailed information can also be found in [14,15]. In section 3.1 the ratio of the slopes of the mean hadron multiplicities in gluon and quark jets with scale is shown to be determined by the colour factor ratio  $C_A/C_F$ . In order to describe the data with the perturbative QCD expectations it is necessary to introduce additional non-perturbative offsets. This analysis is intended to be mainly qualitative and in many aspects it is similar to previous analyses. Then in section 3.2 a precision measurement of the colour factor ratio from symmetric three-jet events is discussed and an estimate for the difference of non-perturbative contributions to the quark and gluon jet multiplicity is given. Finally we summarize and conclude.

## 2 Data Analysis

The analysis presented in this letter uses the full hadronic data set collected with the DELPHI detector (described in [16]) at Z energies in the years 1992 to 1995. The cuts applied to charged and neutral particles and to events in order to select hadronic Z decays are identical to those given in [2] for the  $q\bar{q}g$  analysis and to [8] for the  $q\bar{q}\gamma$  analysis. For the comparison of gluon and quark jets, three-jet events are clustered using the Durham algorithm [17]. In addition it was required that the angles,  $\theta_{2,3}$ , between the low-energy jets and the leading jet are in the range from  $100^\circ$  to  $170^\circ$  (see Fig. 1a)). Within this sample, events are called symmetric if  $\theta_2$  and  $\theta_3$  are equal within some analysis-dependent tolerance. The leading jet is not used in the gluon or quark jet analysis.

The identification of gluon jets by anti-tagging of heavy quark jets is identical to that described in [2,8]. Quark jets are taken from  $q\bar{q}g$  events which have been depleted in b-quark events using an impact parameter technique. In order to achieve multiplicities of pure quark and gluon jet samples, the data have been corrected using purities from simulated events generated with JETSET 7.3 [18] with parameters set as given in [19]. This is justified by the good agreement between data and simulation. Furthermore the model independent techniques described in [2] for symmetric events (see Fig. 1b)) give results largely compatible with those obtained with the simulation correction [15]. The effects of the finite resolution and acceptance of the detector and of the cuts applied are corrected for by using a full simulation of the DELPHI detector [16].

The correction for the remaining b-quark events in the  $q\bar{q}g$  sample does not influence the slope of the measured multiplicity with scale, but only leads to a shift of its absolute value.

In the simulation, quark and gluon jets are identified at “parton level”. The partons entering the fragmentation of a three-jet event are clustered into three jets using the Durham algorithm. Then for each parton jet, the number of quarks and antiquarks are summed where primary quarks contribute with weight +1 and antiquarks with the weight

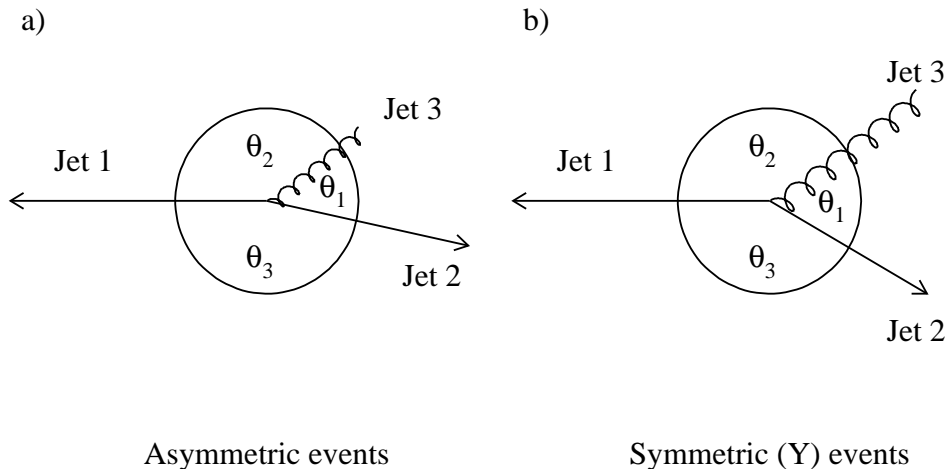


Figure 1: Definition of event topologies and angles used throughout this analysis. The length of the jet lines indicates the energies. In the symmetric (Y) events (see Fig. 1b))  $\theta_2 \approx \theta_3$ .

–1. Other quarks and gluons are assigned the weight 0. These sums are expected to yield +1 for quark jets, –1 for anti-quark jets and 0 for gluon jets. The small amount of events not showing this expected pattern of (+1, –1, 0) was discarded. Finally, the parton jets were mapped to the jets at the hadron level by requiring the sum of angles between the parton and hadron jets to be minimal. Events exceeding a maximum angle between the parton and jet directions were also rejected. At large opening angles the influence of these rejections is found to be about 3% increasing at low opening angles.

The gluon jet purities vary from 95% for low energy gluons to 46% for the highest energy gluons. The few bins with lower purities have been excluded from the analysis. The quark purities range from 43% to 81%.

For the analysis of the multiplicity of symmetric three-jet events, all events were forced to three jets using the Durham algorithm without a minimal  $y_{cut}$ . The angles between the jets were then used to rescale the jet momenta to the centre-of-mass energy as described in [8]. Symmetric events were selected by demanding that  $\theta_2$  be equal to  $\theta_3$  within  $2\epsilon$ . Here  $\epsilon$  is half the angular bin width of  $\theta_1$  taken to be  $3^\circ$ . The analysis has been performed for events of all flavours as well as for b-depleted events. In both cases the measured multiplicity was corrected for track losses due to detector effects and cuts applied. The correction factor was calculated as ratio of generated over accepted multiplicity using simulated events. It varies smoothly, from 1.25 at small  $\theta_1$  to 1.32 at large  $\theta_1$ .

## 3 Results

### 3.1 Comparison of Multiplicities in Gluon and Quark Jets

In order to determine a scale dependence, the scale underlying the physics process needs to be specified. The actual physical scale is necessarily proportional to any variation of an outer scale like the centre-of-mass energy. As usually only the relative change in scale matters, this outer scale can therefore be used instead of the physical scale. For this analysis the situation is different. The jets entering the analysis stem from Z decays

and thus from a fixed centre-of-mass energy. So the relevant scales have to be determined from the properties of the jets and the event topology. From the above discussion the scale has to be proportional to the jet energy because this quantity scales with the energy in the centre-of-mass system for similar events. Studies of hadron production in processes with non-trivial topology have shown that the characteristics of the parton cascade prove to depend mainly on the hardness of the process producing the jet [4,20]:

$$\kappa = E_{jet} \sin \frac{\theta}{2} \quad . \quad (1)$$

$E_{jet}$  is the energy of the jet and  $\theta$  its angle to the closest jet. This scale definition corresponds to the beam energy in two-jet events. It is similar to the transverse momentum of the jet and also related to  $\sqrt{y_{cut}}$  as used by the jet algorithms. It is also used as the scale in the calculation of the energy dependence of the hadron multiplicity in  $e^+e^-$  annihilation [21,22] to take into account the leading effect of coherence. It should, however, be noted that several scales may be relevant in multi-jet events. Hence using  $\kappa$  is an approximation. A similar scale, namely the geometric mean of the scales of the gluon jet with respect to both quark jets while using Eqn. 1 for the quark jets, has recently been used in a study of quark and gluon jet multiplicities [12].

As stated in the introduction we want to gain information on the relative colour charges of quarks and gluons from the rate of change of the multiplicities with scale. Assuming the validity of the perturbative QCD prediction, the ratio of the charged multiplicities of gluon and quark jets,  $N_{gluon}/N_{quark}$ , has to approach a constant value (approximately the colour factor ratio) at large scale. This trivially implies that the ratio of the slopes of quark and gluon jet multiplicities also approaches the same limit. This fact is a direct consequence of de l'Hôpital's rule [23] and is also directly evident from the linearity of the derivative:

$$\text{at large scale: } N_{gluon}(\kappa) = C \cdot N_{quark}(\kappa) \quad \rightarrow \quad \frac{dN_{gluon}/d\kappa}{dN_{quark}/d\kappa} = C \quad , \quad (2)$$

i.e. the QCD prediction for the ratio of multiplicities applies equally well to the ratio of the slopes of the multiplicities. In fact it is to be expected that the slope ratio is closer to the QCD prediction than the multiplicity ratio as it should be less affected by non-perturbative effects.

This effect has been cross-checked using the HERWIG model [24] which allows the number of colours to be changed and thus by SU(n) group relations, the colour factor ratio  $C_A/C_F$ . The predictions of HERWIG are found to follow directly the expectation of the right hand side of Eqn. 2. This has also been confirmed in a recent theoretical calculation of this quantity [25] in the framework of the dipole model.

Fig. 2a) shows the multiplicity in quark and gluon jets as a function of the hardness scale  $\kappa$ . For both multiplicities an approximately logarithmic increase with  $\kappa$  is observed which is about twice as big for gluon jets as for quark jets, thus already strikingly confirming the QCD prediction.

A stronger increase of the gluon jet multiplicity was already noted in a previous paper [8], where the jet energy was chosen as scale. Meanwhile this observation has been confirmed also by other measurements [9–11] and has been extended to different scales [12]. Fragmentation models (not shown) predict an increase of the multiplicities which is in good agreement with the data.

In order to obtain quantitative information from the data shown in Fig. 2a), the following ansatz was fitted to the data:

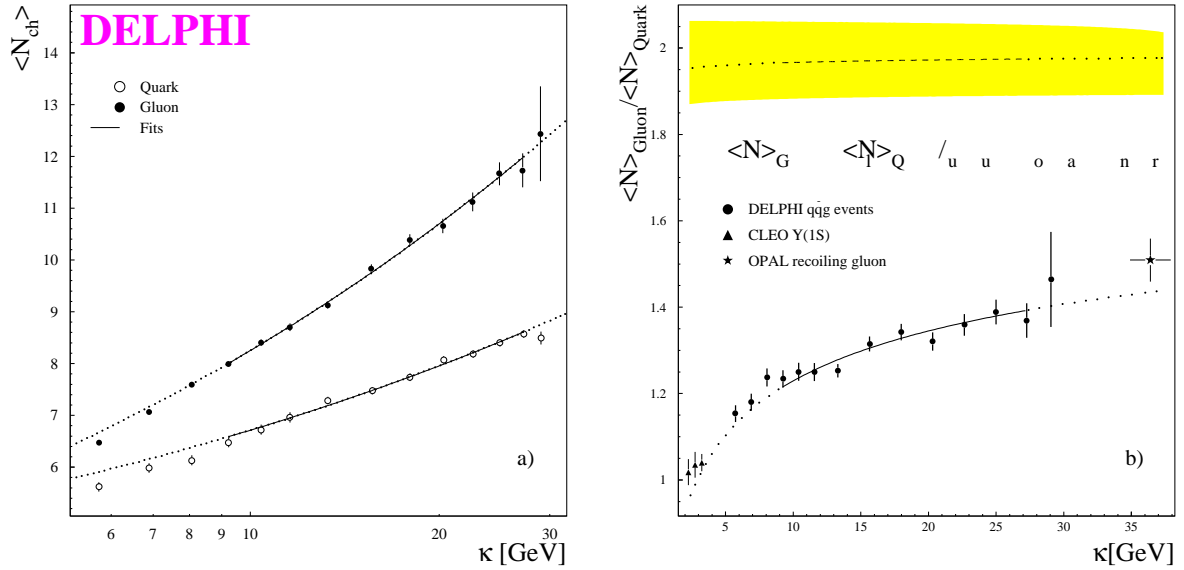


Figure 2: a) Average charged particle multiplicity for light quark and gluon jets as function of  $\kappa$  fitted with Eqn. 3; b) ratio of the gluon to quark jet multiplicity; the full line shows the ratio of the functions fitted to the data in a), the dashed curve is the ratio of the slopes of the fits in a). All curves are extrapolated to the edges of the plot by the dotted lines. Also included are measurements of the multiplicity ratio of some other experiments [10,11]. The grey band shown with the slope ratio indicates the error estimated by varying all fit parameters within their errors.

$$\begin{aligned} \langle N_q \rangle (\kappa) &= N_0^q + N_{pert}(\kappa) \\ \langle N_g \rangle (\kappa) &= N_0^g + N_{pert}(\kappa) \cdot r(\kappa) \end{aligned} \quad (3)$$

Here  $N_0^{q,g}$  are non-perturbative terms introduced to account for the differences in the fragmentation of the leading quark or gluon as discussed in detail in the introduction. These terms are assumed to be constant.  $N_{pert}$  is the perturbative prediction for the hadron multiplicity as given in [21]:

$$N_{pert}(\kappa) = K \cdot (\alpha_s(\kappa))^b \cdot \exp\left(\frac{c}{\sqrt{\alpha_s(\kappa)}}\right) \cdot [1 + O(\sqrt{\alpha_s})] \quad (4)$$

$$b = \frac{1}{4} + \frac{2n_f}{3\beta_0} \left(1 - \frac{C_F}{C_A}\right) \quad ; \quad c = \frac{\sqrt{32C_A\pi}}{\beta_0} \quad ; \quad \beta_0 = 11 - \frac{2}{3}n_f \quad .$$

A first and a second order  $\alpha_s$  have been used with this expression with the number of active flavours,  $n_f$ , equal to five. An alternative prediction has been given in [26] using the limited spectrum approach:

$$N_{pert} = K \cdot \Gamma(B) \left(\frac{z}{2}\right)^{1-B} I_{1+B}(z) \quad (5)$$

$$B = \frac{33 + 2/9n_f}{33 - 2n_f} \quad ; \quad z = \log \frac{\kappa^2}{\Lambda^2} \gamma_0 \quad ; \quad \gamma_0 = \sqrt{\frac{2}{\pi} C_A \alpha_s(\kappa)}$$



Here a first order  $\alpha_s$  has always been used with  $n_f$  taken as three [27].  $\Gamma$  is the Gamma-function and  $I_B$  the modified Bessel-function.  $K$  is a non-perturbative scale factor. The QCD scale parameter  $\Lambda$  enters into the definition of  $\alpha_s(\kappa^2/\Lambda^2)$  [22]. The numerical values of  $K$  and  $\Lambda$  are not expected to be the same in Eqns. 4 and 5 as different approximations are used. Finally:

$$r(\kappa) = \frac{C_A}{C_F}(1 - r_1\gamma_0 - r_2\gamma_0^2) \quad (6)$$

with:

$$r_1 = \frac{1}{6} \left( 1 + \frac{n_f}{C_A} - \frac{2n_f C_F}{C_A^2} \right) ; \quad r_2 = \frac{r_1}{6} \left( \frac{25}{8} - \frac{3}{4} \frac{n_f}{C_A} - \frac{n_f C_F}{C_A^2} \right)$$

is the perturbative prediction [28] for the multiplicity ratio in back-to-back gluon to back-to-back quark jets. The terms proportional to  $r_1$  ( $r_2$ ) correspond to the NLO (NNLO) prediction. Numerically they correspond to corrections of about 8% and 1% respectively. The smallness of the higher order corrections indicates that the perturbative series of the gluon-to-quark multiplicity ratio converges rapidly.

The fits represent the data well. The fit range has not been extended to too small scales as here a contribution of initial two-jet events might bias the multiplicities to lower values. Parameters of the fits for this specific choice of scale and jet selection are given in Tab. 1. No estimate of systematic error is given as this analysis is intended to be mainly qualitative. The fit parameters should not be compared directly to those parameters usually obtained from overall events in  $e^+e^-$  annihilation. The normalization factor,  $K$ , differs strongly due to the differences in the multiplicity in jets and overall events. Furthermore, the introduction of non-perturbative offsets leads to a strong reduction of the values of the effective scale parameter  $\Lambda$ . This is also observed if the  $e^+e^-$  multiplicity is fitted including an offset term, which could be reasonable in this case also.

Parameter	$N_{pert}$ from Eqn. 4	$N_{pert}$ from Eqn. 5
$\Lambda$ [GeV]	$0.032 \pm 0.011$	$0.011 \pm 0.004$
K	$0.005 \pm 0.001$	$0.12 \pm 0.02$
$C_A/C_F$	$2.12 \pm 0.10$	$2.15 \pm 0.10$
$N_0^q$	$2.82 \pm 0.14$	$3.12 \pm 0.20$
$N_0^g$	$0.73 \pm 0.21$	$1.43 \pm 0.31$
$\chi^2/\text{n.d.f.}$	0.61	0.65

Table 1: Results of the fits of the quark and gluon jet multiplicities as a function of  $\kappa$ .

Using an identical scale definition for quark and gluon jets also allows the gluon-to-quark jet multiplicity ratio to be directly evaluated as function of this scale. Fig. 2b) shows this ratio as calculated from data and the fits as function of the hardness scale as well as the ratio of the slopes of the fits. The ratio of the multiplicities increases from about 1.15 at small scale to about 1.4 at the highest scales measured. The measurement [10] performed in  $\Upsilon(1S) \rightarrow \gamma gg$  decays at small scale<sup>1</sup>, and of “inclusive” gluons [11] at large scale, agree quite well with the expectation from the fits. The corresponding hardness scale for the data at the highest scale [11] has been estimated from the average

<sup>1</sup>Half of the  $gg$  invariant mass is taken as the equivalent scale.

gluon energy and the angle cuts given in [11]. The good agreement of the “inclusive” gluon measurement also implies that angular ordering effects are relevant in this case.

The ratio of the slopes for the different fits is almost 2 corresponding to a colour factor ratio of  $C_A/C_F = 2.12 \pm 0.10$ , well compatible with the QCD expectation.

The fits further indicate that for very small scale the multiplicity of quark jets is bigger than that of gluon jets. Consequently the constant terms contributing to the multiplicity due to the primary gluon or quark fragmentation are larger for quarks (see Tab. 1). The difference of these terms is about 2. Taking the scale choice made in [12] leads to about a 20% increase of the measured colour factor ratio and a corresponding increase in the difference of the non-perturbative constants to 4.2.

It is instructive here to estimate a lower limit for the difference of the non-perturbative terms from the behaviour of the gluon and quark fragmentation functions [2]. Due to leading particle effects the fragmentation function of the quark outreaches the fragmentation function of the gluon at high values of  $x_E$ . Taking the shape of the gluon fragmentation function as unbiased by the leading particle effect and assuming the overall multiplicity of gluon jets roughly as twice as big as of quark jets, one gets an estimate for the lower limit of additional multiplicity in quark jets by integrating the difference between the quark and the halved gluon fragmentation function in the  $x_E$ -region where the fragmentation function of the gluon is below that of the quark. This yields  $N_0^q - N_0^g \geq 0.61 \pm 0.02$  from Y and  $N_0^q - N_0^g \geq 0.58 \pm 0.05$  from so-called Mercedes events [2]. It should be noted here, that the leading particle effect still influences the multiplicity at even lower scaled hadron energies. The region of small hadron energy contributes most to the multiplicity. Therefore the estimated limit presumably is much smaller than the actual value of  $N_0$ .

At first sight a difference of the constant terms of the order of  $\sim 2$  units in charged multiplicity looks unexpectedly large. However, these constants also include the effects of the jet clustering. Furthermore, stable hadron production to a large extent proceeds via resonance decays, so that the observed difference may only correspond to a difference of about one primary particle. The larger constant term for quarks compared to gluons explains the different behaviour of the ratio of multiplicities and the slope ratio in Fig. 2b).

The observed behaviour would be expected from non-perturbative effects of the fragmentation in the leading quark or gluon. In the cluster fragmentation model, an additional gluon to quark-antiquark splitting is needed in the fragmentation of a gluon compared to that of a quark.

### 3.2 Precise Determination of $C_A/C_F$ from Multiplicities in Three-Jet Events

The analysis presented so far, as in most other comparisons of quark and gluon jet multiplicities, has the disadvantage of relying on the association of (maybe low energy) particles to jets. Clearly this involves severe ambiguities and specifically does not consider coherent soft gluon radiation from the initial  $q\bar{q}g$  ensemble. This can be avoided and a precise measurement can be obtained by studying the dependence of the total charged multiplicity in three-jet events as function of the quark and gluon scales. In fact there is a definite MLLA prediction [13] for this multiplicity  $N_{q\bar{q}g}$ :

$$N_{q\bar{q}g} = \left[ 2N_q(Y_{q\bar{q}}^*) + N_g(Y_g^*) \right] \cdot \left( 1 + \mathcal{O}\left(\frac{\alpha_s}{\pi}\right) \right) \quad (7)$$

with the scale variables:

$$Y_{q\bar{q}}^* = \ln \sqrt{\frac{p_q p_{\bar{q}}}{2\Lambda^2}} = \ln \frac{E^*}{\Lambda} \quad , \quad Y_g^* = \ln \sqrt{\frac{(p_q p_g)(p_{\bar{q}} p_g)}{2\Lambda^2(p_q p_{\bar{q}})}} = \ln \frac{p_1^\perp}{2\Lambda} \quad , \quad (8)$$

$N_q(Y_{q\bar{q}}^*)$  and  $N_g(Y_g^*)$  describe the scale dependence of the multiplicity for quark or gluon jets, respectively.  $\Lambda$  is a scale parameter and the  $p_{q,\bar{q},g}$  are the four-momenta of the quarks and the gluon. The three-jet multiplicity depends on the quark energy,  $E^*$ , in the centre-of-mass system of the quark-antiquark pair and on the transverse momentum scale of the gluon,  $p_1^\perp$ . For comparison with data, this is expressed in [29] as a dependence on the measured multiplicity in  $e^+e^-$  events,  $N_{e^+e^-}$ , and the colour factor ratio as given in Eqn. 6. In addition, we again choose to add a constant term,  $N_0$ , to account for differences in the fragmentation of quarks and gluons as discussed above. Thus, omitting correction terms:

$$N_{q\bar{q}g} = N_{e^+e^-}(2E^*) + r(p_1^\perp) \left\{ \frac{1}{2} N_{e^+e^-}(p_1^\perp) - N_0 \right\} \quad . \quad (9)$$

Although at first sight this appears to be the incoherent sum of the multiplicity of the two quark jets and the gluon jet, this formula includes coherence effects in the exact definition of the scales of the  $N_{e^+e^-}$  terms [27]. Nevertheless, subtracting the non-perturbative term  $N_0$  within the curly brackets gives a physical interpretation for  $N_0$  as the additional multiplicity in quark jets due to the leading particle effect, which is contained in the measured  $N_{e^+e^-}$  and has to be subtracted to get the gluon contribution to the multiplicity.

In principle Eqn. 9 still requires the determination of the quark-antiquark and gluon scales independently. However, in symmetric Y-type events (see Fig. 1b)) both scales can be expressed as functions of the opening angle  $\theta_1$  only by initially assuming that the gluon jet is not the most energetic one.  $E^{*2} \propto E_q E_{\bar{q}} \sin^2 \theta_3/2$  for this type of event is almost constant (see upper full curve in Fig. 3a)) at fixed centre-of-mass energy. However,  $p_1^\perp$ , increases approximately linearly with the opening angle as it is proportional to the gluon transverse momentum. As the multiplicity change corresponding to the change of  $E^*$  corresponds only to about  $-2$ , the  $\theta$  dependence of the three-jet multiplicity therefore mainly measures the scale dependence of the multiplicity of the gluon jet.

In a fraction of the events (which strongly increases with opening angle) the gluon jet is the most energetic jet. This can be corrected for in different ways when fitting Eqn. 9 to the data using Monte Carlo simulation. Assuming an approximately logarithmic increase of the multiplicity with scale, which is well supported by the data, the average scale at a given opening angle can be expressed as the geometric mean of the cases where the gluon initiates the most energetic jet and where it does not. These corrected scales are shown as the points in Fig. 3a). The correction first increases with the opening angle but then decreases again and vanishes for fully symmetric events. Alternatively, the fraction of events when the gluon initiates the most energetic jet can be considered separately in Eqn. 9.

To obtain information on the colour factor ratio  $C_A/C_F$ , the scale dependence of the three-jet multiplicity has to be compared to the multiplicity in all  $e^+e^-$  events. This has been chosen to be taken from the DELPHI measurements with hard photon radiation for energies below the Z mass and at 184 GeV [30] and the LEP combined measurements at the intermediate energies [31]. For studies of systematic errors, data from lower energy  $e^+e^-$  experiments [32] have also been used. The DELPHI multiplicities in events with hard photon radiation have been extracted as described in [8,14], but using the full statistics now available. Small energy dependent corrections ( $2 - 4\%$ ) to the  $e^+e^-$

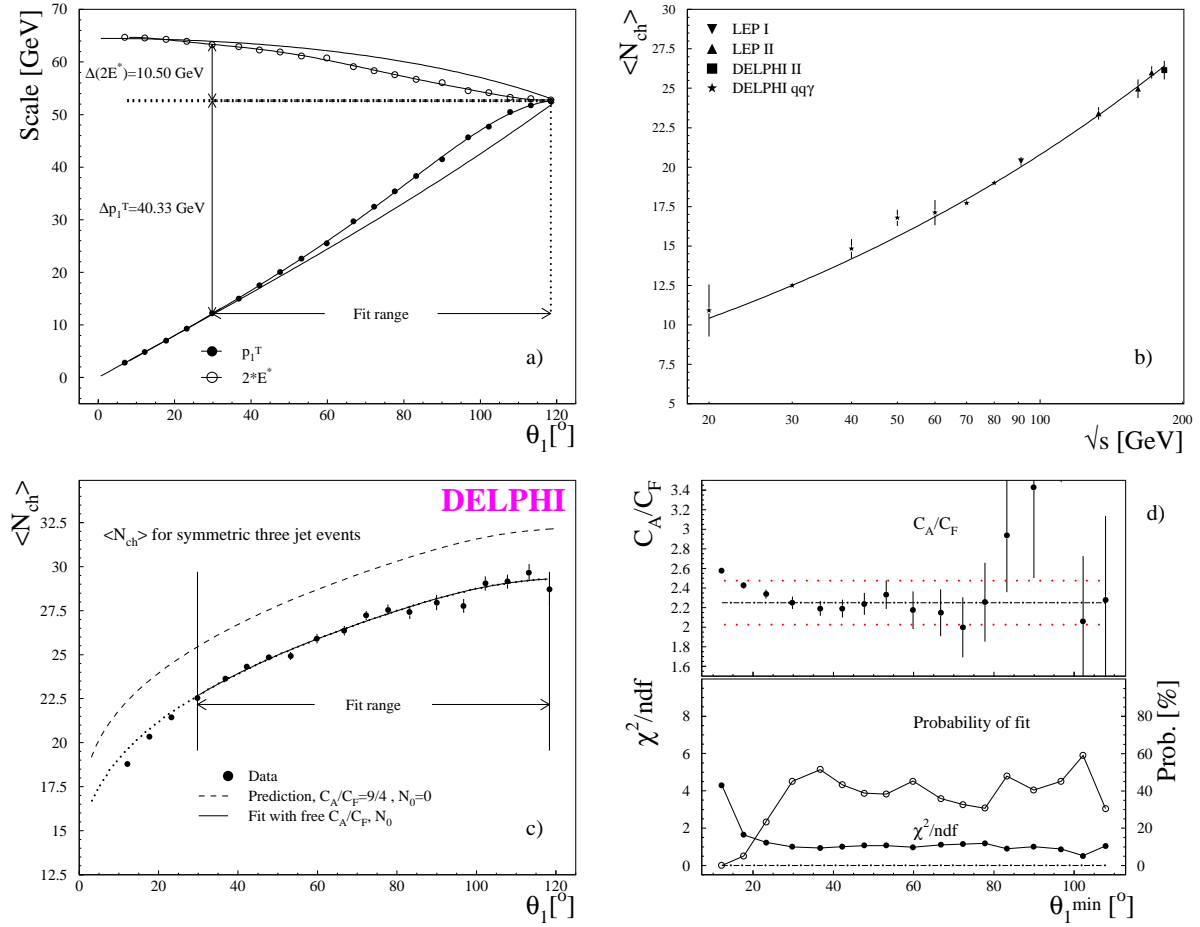


Figure 3: a) Variation of the scales  $2E^*$  and  $p_1^\perp$  as function of the opening angle  $\theta_1$  in symmetric three-jet events. The functions are the analytic expectation. The points include a correction (calculated with JETSET 7.3) for the cases where the gluon forms the most energetic jet. The lines matching the points are polynomials fitted to obtain continuous values.

b) Charged hadron multiplicity as a function of the centre-of-mass energy of the  $q\bar{q}$ -pair fitted with the perturbative predictions Eqs. 4 or 5.

c) Charged hadron multiplicity in symmetric three-jet events as a function of the opening angle. The dashed curve is the prediction using the ansatz Eqn. 9 setting  $C_A/C_F$  to its default value and omitting the constant offset,  $N_0$ . The full curve is a fit of the full ansatz Eqn. 9 to the data treating  $C_A/C_F$  and  $N_0$  as free parameters.

d) Stability of the result for  $C_A/C_F$  against variation of the smallest opening angle used in the fit as well as  $\chi^2/N_{df}$  and the  $\chi^2$  probability of these fits. The dash-dotted horizontal line in the upper half shows the QCD expectation for  $C_A/C_F$  with the dotted lines representing variations of  $\pm 10\%$ .

The DELPHI data of Fig. 3 b) and c) will be made available in the Durham/RAL database [38].

multiplicities were applied to correct for the varying contribution of b quarks. The multiplicities obtained were fitted with the perturbative predictions, Eqs. 4 or 5, see Fig 3b). Both calculations describe the data equally well. The parameters of the fits are given in the upper part of Tab. 2.

Parameter	$N_{pert}$ from [21] (Eqn.4)	$N_{pert}$ from [26] (Eqn.5)	relevant data
$\Lambda$	$0.275 \pm 0.070$	$0.061 \pm 0.015$	data from $e^+e^-$ and $q\bar{q}\gamma$
K	$0.026 \pm 0.003$	$0.606 \pm 0.062$	
$\chi^2/\text{n.d.f.}$	1.180	1.183	
$C_A/C_F$	$2.251 \pm 0.063$	$2.242 \pm 0.062$	data from symmetric 3 jet events
$N_0$	$1.40 \pm 0.10$	$1.40 \pm 0.10$	
$\chi^2/\text{n.d.f.}$	0.998	1.004	

Table 2: Result of the fits of the  $e^+e^-$  multiplicity (upper part) and the three-jet event multiplicity (lower part).

The measured, fully corrected multiplicity in all symmetric three-jet events as function of the opening angle is shown in Fig. 3c). A strong increase of the multiplicity from values of around 18 for small opening angle to about 29 at opening angles of  $120^\circ$  (corresponding to fully symmetric events) is observed. Omitting the non-perturbative term,  $N_0$ , in Eqn. 9 and setting  $C_A/C_F$  to its expected value predicts a similar increase in multiplicity over this angular range (dashed curve in 3c)). The prediction is however higher by about three units of charged multiplicity. This discrepancy is expected from the previously obtained result due to differences in the fragmentation of the leading quark or gluon.

At small angles the difference between the primary QCD expectation and the measurement increases. Studies using Monte Carlo models have shown that this is mainly due to genuine two jet events which have been clustered as symmetric three-jet events. The models indicate that this contribution becomes small for angles above  $30^\circ$ .

Fitting the full ansatz 9 to the three-jet multiplicity data at angles  $\theta \geq 30^\circ$ , using the two parameterizations in Eqs. 4 and 5 of the multiplicity in  $e^+e^-$  events with their parameters fixed as given in Tab. 2 but varying  $C_A/C_F$  and  $N_0$ , yields:

$$\frac{C_A}{C_F} = 2.251 \pm 0.063 \quad (10)$$

$$\frac{C_A}{C_F} = 2.242 \pm 0.062. \quad (11)$$

The result confirms with great precision the QCD expectation [1] that the ratio of the radiated multiplicity from gluon and quark jets is given by the colour factor ratio  $C_A/C_F$ . This result also implies that the proportionality of the number of gluons to hadrons [1] e.g. Local Hadron Parton Duality (LPHD) [33] applies extremely precisely if only the radiated gluons from a quark or gluon are considered.

The offset term  $N_0$  is bigger if only b-depleted events are used. The central result for  $C_A/C_F$ , however, remains unchanged within errors. This is due to the fact that  $C_A/C_F$  is measured from the change of multiplicity in three-jet events with opening angle and not from the absolute multiplicity.

The correctness of the ansatz Eqn. 9 and the bias introduced by two-jet events at small  $\theta_1$ , were further checked by varying the lowest angle used in the fit. The resulting

value for  $C_A/C_F$ , the  $\chi^2/N_{df}$  and the  $\chi^2$  probability of the fit are shown in Fig. 3d). It is observed that for  $\theta_1 > 30^\circ$  satisfactory fits are obtained. For this angular range the fitted value of  $C_A/C_F$  is stable within errors.

Systematic uncertainties of the above result for the colour factor ratio due to uncertainties in the three-jet multiplicity data as well as in the parameterization of the  $e^+e^-$  charged multiplicity and in the theoretical predictions are considered. To obtain systematic errors interpretable like statistical errors, half the difference in the value obtained for  $C_A/C_F$  when a parameter is modified from its central value (see below) is quoted as the systematic uncertainty. All relative systematic errors are collected in Tab. 3.

Source	Sys. error	combined	combined	total	
Experimental uncertainties					
1. Min. particle momentum	$\pm 0.42 \%$			$\pm 5.52\%$	
2. Min. angle of jet w.r.t. beam	$\pm 0.38 \%$				
3. Min. number of tracks per jet	$\pm 0.02 \%$	$\pm 0.58\%$			
4. Corr. for gluon in jet 1	$\pm 0.11 \%$				
5. jet algorithms		$\pm 1.39 \%$	$\pm 3.55 \%$		
6. $e^+e^-$ data sets	$\pm 0.90 \%$				
7. Fit function	$\pm 0.02 \%$	$\pm 3.21 \%$			
8. binning and range of fit	$\pm 3.08 \%$				
Theoretical uncertainties					
9. Variation of $n_f$	$\pm 1.51 \%$				
10. Calculation in 1st/2nd order	$\pm 3.95 \%$		$\pm 4.23\%$		
11. Setting $C_A$ fixed	$\pm 0.08 \%$				

Table 3: Systematic uncertainties on  $C_A/C_F$  as derived from three-jet event multiplicities

Results for  $C_A/C_F$  obtained from the individual data sets corresponding to the different years of data-taking as well as from b-depleted events were found to be fully compatible within the statistical error. To estimate uncertainties in the three-jet multiplicity the following cuts which are sensitive to misrepresentation of the data by the Monte Carlo simulation have been varied.

1. Cut on the minimal particle momentum:  
the cut on the minimal particle momentum has been lowered from 400 MeV to 200 MeV and raised to 600 MeV.
2. Minimum angle of each jet with respect to the beam axis:  
this cut has been increased from  $30^\circ$  to  $40^\circ$  to test for a possible bias due to the limited angular acceptance.
3. Minimum number of particles per jet:  
the minimum number of particles per jet has been increased from 2 to 4 in order to reject events which may not have a clear three-jet structure.
4. Correction for gluon in leading jet:  
both methods of correction were compared to account for gluons in the most energetic jet. Furthermore the requirements for the mapping of the parton to the hadron level for defining the gluon jet have been varied.

To check the stability of the result for different choices of jet algorithms the results obtained for a large sample of events generated with JETSET have been compared with:

5. Alternative jet algorithms:

the angular ordered Durham algorithm, LUCLUS without particle reassignment, JADE and Geneva [34] were applied alternatively to Durham on a large statistics Monte Carlo sample. The results for Durham, angular ordered Durham and LUCLUS agree reasonably. The spread among the results was taken as error. The JADE and Geneva algorithm which are known to tend to form so-called junk jets [34] show stronger deviations.

The following systematic uncertainties arise from uncertainties in the experimental input other than from the three-jet multiplicities and from choices made for the fits of  $N_{e^+e^-}$ . These uncertainties are considered as experimental systematic uncertainties.

6. Input of parameterization of  $N_{e^+e^-}(\sqrt{s})$ :

to estimate the influence of an uncertainty in  $N_{e^+e^-}$ , different choices of input data were compared:

- DELPHI multiplicities for 184 GeV and from Z decays with hard photons combined with LEP data for  $90 \text{ GeV} < \sqrt{s} < 180 \text{ GeV}$  ;
- DELPHI multiplicities from Z decays with hard photons;
- $e^+e^-$  data taken at low centre-of-mass energies (TASSO, TPC, MARK-II, HRS, AMY);
- all available  $e^+e^-$  data between 10 GeV and 184 GeV (TASSO, TPC, MARK-II, HRS, AMY, LEP combined, DELPHI).

7. Choice of prediction used for fit:

the fit functions 4 and 5 were used alternatively. For consistency here  $n_f = 5$  and a second order  $\alpha_s$  was used.

8. Variation of the fitted range:

the lower limit of the angular range used in the fit was varied between  $24^\circ$  and  $36^\circ$  as well as changing half the bin width,  $\epsilon$ , from  $2.5^\circ$  to  $5^\circ$ .

Finally, systematic errors due to uncertainties in the theoretical prediction were considered.

9. Variation of  $n_f$ :

the number of active quarks,  $n_f$ , [22] relevant for the hadronic final state is uncertain.  $n_f$  therefore has been varied from 3 to 5.

10. Order of calculation (LO - NNLO):

the prediction  $r(\kappa)$  (Eqn. 6) has been calculated for back-to-back quarks or gluons. As the jets are well separated it is expected to apply for this analysis also. When the gluon recoils with respect to the quarks the prediction is exact. In addition coherence effects (angular ordering) are taken into account in the definition of the scales  $E^*$  and  $p_1^\perp$ .

As the coupling for the triple-gluon vertex is bigger than the coupling of all other vertices it is clear that the correction will lower the gluon-to-quark multiplicity ratio as in the case of Eqn. 6. The validity of the correction [28] is therefore assumed for the whole range of angles considered. Conservatively, half of the difference obtained with the lowest order prediction  $r = C_A/C_F$  and the NNLO prediction is considered as systematic uncertainty. A leading order  $\alpha_s$  was used for the lowest order prediction and a second order  $\alpha_s$  in the other case. Considering that in the three-jet events mainly the gluon scale  $p_1^\perp$  is varied, the resulting error estimate agrees with that given in Eqn. 7.

### 11. Quantities influencing $C_A/C_F$ :

for the central result,  $C_A/C_F$  has been assumed variable in Eqn. 6 only. The stability of the result was checked by also leaving  $C_A$  variable in some or all of the parameterizations of  $\alpha_s$  and  $N_{e^+e^-}$ .

To check in how far the offset term  $N_0$  is constant,  $N_0$  has been extracted for each  $\theta_1$ -bin individually fixing  $C_A$  to its default value. The individual results are consistent with the average value and no trend is observed.

Alternatively to Eqn. 9, Eqn. 7 has been fitted to the data, where the  $\mathcal{O}(\alpha_s)$  correction factor has been parameterized as  $(1 + c\alpha_s(p_1^\perp))$ . This leads to the same fit results for  $C_A/C_F$  and  $\chi^2$  as Eqn. 9, which implies that both corrections  $r(p_1^\perp) \cdot N_0$  and  $[2N_q(Y_{q\bar{q}}^*) + N_g(Y_g^*)] \cdot c\alpha_s(p_1^\perp)$  as well as the values obtained for  $C_A/C_F$  agree within  $\pm 1\%$ . It should, however, be stressed that the behaviour of the fragmentation function requires the presence of a non-perturbative offset term.

The prediction of the multiplicity ratio given by [35] has been tried as an alternative to Eqn. 6. Although this calculation takes recoil effects into account, a non-perturbative offset term is still required. The prediction differs by about 10% from [28] in the NNLO term. As it does not reproduce the colour factor ratio contained in the fragmentation models which describe the data well, it has not been applied in this analysis.

Averaging the results given in Eqns. 10 and 11 and adding in quadrature the systematic errors summarized in Tab. 3 gives the following final result:

$$\frac{C_A}{C_F} = 2.246 \pm 0.062 \text{ (stat.)} \pm 0.080 \text{ (syst.)} \pm 0.095 \text{ (theo.)} \quad (12)$$

This result confirms the QCD expectation that gluon bremsstrahlung is stronger from gluons than from quarks by the colour factor ratio  $C_A/C_F$  and is direct evidence for the triple-gluon coupling.

This measurement yields the most precise result obtained so far for the colour factor ratio  $C_A/C_F$ . Even the best measurements from four-jet angular distributions [36] suffer from the relatively small number of four-jet events available. Furthermore, many of these measurements specify no theoretical systematic error as they so far rely on leading order calculations. It is remarkable that this measurement of  $C_A/C_F$  is performed from truly hadronic quantities, the charged multiplicities. Jets, i.e. partonic quantities only enter indirectly via the definition of the scales  $E^*$  and  $p_1^\perp$ .

In order to illustrate comprehensively the contents of the measurement of the three-jet multiplicity we compare in Fig. 4 the multiplicity corresponding to a  $gg$  and a  $q\bar{q}$  final state. The  $q\bar{q}$  multiplicity is taken to be the multiplicity measured in  $e^+e^-$  annihilation corrected for the  $b\bar{b}$  contribution as described above. The  $gg$  multiplicity at low scale values is taken from the CLEO measurement [10], for which no systematic error was specified. At higher scale, twice the difference of the three-jet multiplicity and the  $q\bar{q}$  term (the first term in Eqn. 9) is interpreted as the  $gg$  multiplicity. The  $gg$  data should be extendable to higher energies by measuring the multiplicity in  $p\bar{p}$  scattering as a function of the transverse energy. The dashed curve through the  $q\bar{q}$  points is a fit of the prediction according to Eqns. 4 or 5. The  $gg$  line is the perturbative expectation for back-to-back gluons according to the second term of Eqn. 9.  $N_0$  is taken from Eqn. 13. In principle  $N_0$  is a property of the complete three-jet event, so it is unclear if the subtraction of the full amount of  $N_0$  is justified in order to obtain the gluon jet multiplicity. However, this only introduces a constant shift in the “ $gg$  event” multiplicity, the scale dependence of the gluon jet multiplicity remains unaltered. The plot shows again that the increase of



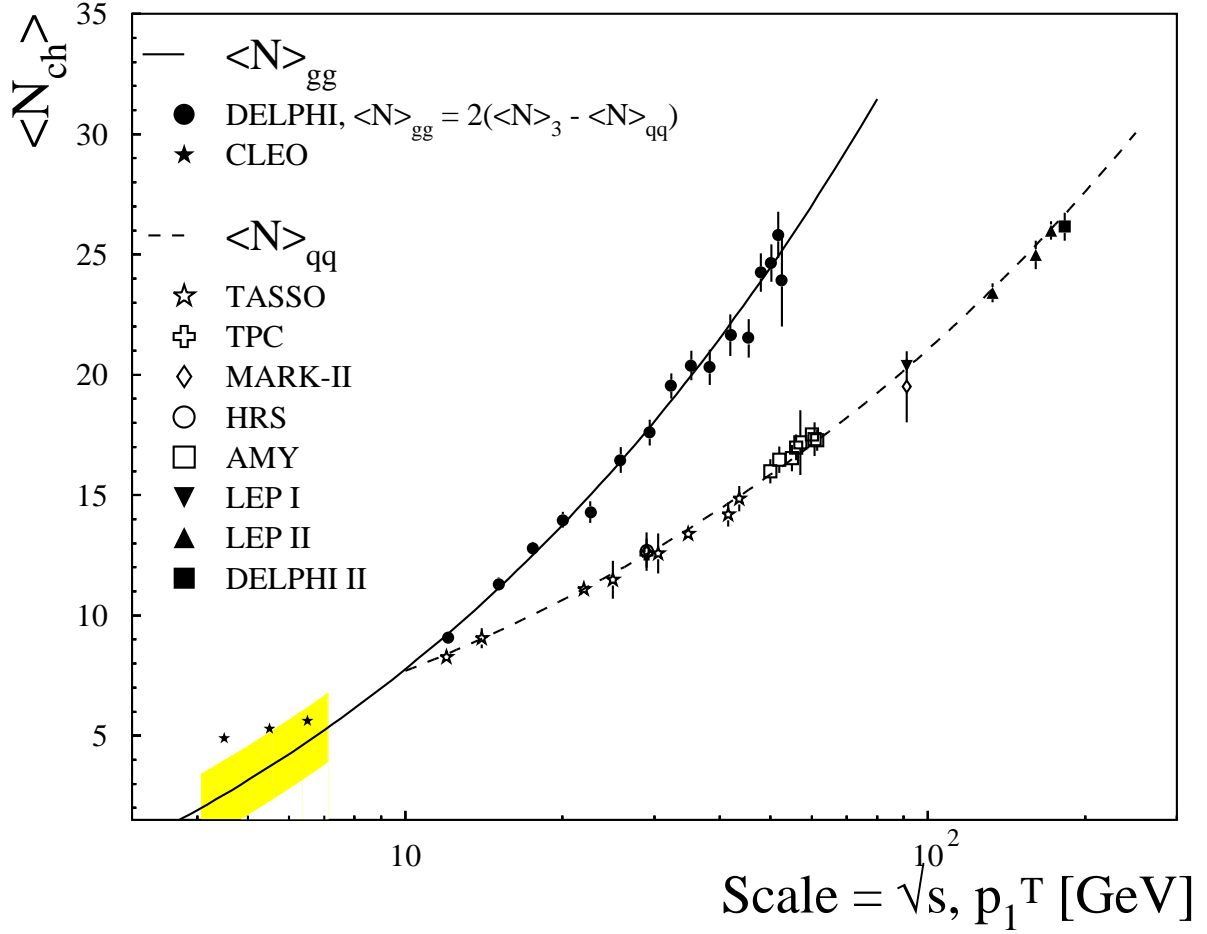


Figure 4: Comparison of the charged hadron multiplicity for an initial  $q\bar{q}$  and a  $gg$  pair as function of the scale. The dashed curve is a fit according to Eqns. 4 or 5, the full line is twice the second term of Eqn. 9. The grey band indicates the uncertainty due to the error of  $N_0$ . The DELPHI  $gg$  data will be made available in the Durham/RAL database [38].

the  $gg$  multiplicity with scale is about twice as big as in the  $q\bar{q}$  case, illustrating the large gluon-to-quark colour factor ratio  $C_A/C_F$ .

It is of interest to present also a dedicated measurement of the non-perturbative parameter  $N_0$ . In order to obtain this value, b-depleted events have been used. A fit of the three-jet event multiplicity has then been performed with  $N_0$  as the only free parameter.  $C_A/C_F$  has been set to its default value. The parameterization of the  $e^+e^-$  multiplicity according to Eqn. 4 uses the low energy  $e^+e^-$  data as input. The fit yields:

$$N_0 = 1.91 \pm 0.03(stat.) \pm 0.33(syst.) \quad (13)$$

The systematic error was estimated as for  $C_A/C_F$ . Furthermore a normalization error due to the multiplicity in  $e^+e^-$  events has been added in quadrature. This error has been assumed to be given by the error of the precise average multiplicity at the Z resonance [37]. The actual value of  $N_0 \approx 2$  corresponds to about one primary particle (see also section 3.1). This is indeed a reasonable value which had already been expected in [1].

## 4 Summary

In summary, the dependence of the charged particle multiplicity in quark and gluon jets on the transverse momentum-like scale has been investigated and the charged hadron multiplicity in symmetric three-jet events has been measured as a function of the opening angle  $\theta_1$ .

The ratio of the variations of gluon and quark jet multiplicities with scale agrees with the QCD expectation and directly reflects the higher colour charge of gluons compared to quarks. This can also be interpreted as direct evidence for the triple-gluon coupling, one of the basic ingredients of QCD. It is of special importance that this evidence is due to very soft radiated gluons and therefore complementary to the measurement of the triple-gluon coupling in four-jet events at large momentum transfer.

The increase of the gluon to quark jet multiplicity ratio with increasing scale is understood as being due to a difference in the fragmentation of the leading quark or gluon. The simultaneous description of the quark and gluon jet multiplicities with scale also supports the Local Parton Hadron Duality hypothesis [33] although large non-perturbative terms for the leading quark or gluon are responsible for the observed relatively small gluon to quark jet multiplicity ratio.

Using the novel method of measuring the evolution of the multiplicity in symmetric three-jet events with their opening angle, a precise result for the colour factor ratio is obtained:

$$\frac{C_A}{C_F} = 2.246 \pm 0.062 \text{ (stat.)} \pm 0.080 \text{ (syst.)} \pm 0.095 \text{ (theo.)}$$

It is superior in precision to the best measurements from four-jet events [36]. Finally it is remarkable that this measurement is directly performed from truly hadronic quantities. Jets only enter indirectly via the definition of the energy scale of the quark-antiquark pair and the transverse momentum scale of the gluon. These scales are calculated directly from the jet angles.

## Acknowledgements

We would like to thank V.A. Khoze for his interest in this analysis and many enthusiastic discussions and explanations. We thank S. Lupia and W. Ochs for providing us with their program for Eqn. 5.

We are greatly indebted to our technical collaborators, to the members of the CERN-SL Division for the excellent performance of the LEP collider and to the funding agencies for their support in building and operating the DELPHI detector.

We acknowledge in particular the support of:

Austrian Federal Ministry of Science and Traffics, GZ 616.364/2-III/2a/98,

FNRS-FWO, Belgium,

FINEP, CNPq, CAPES, FUJB and FAPERJ, Brazil,

Czech Ministry of Industry and Trade, GA CR 202/96/0450 and GA AVCR A1010521,

Danish Natural Research Council,

Commission of the European Communities (DG XII),

Direction des Sciences de la Matière, CEA, France,

Bundesministerium für Bildung, Wissenschaft, Forschung und Technologie, Germany,

General Secretariat for Research and Technology, Greece,

National Science Foundation (NWO) and Foundation for Research on Matter (FOM),

The Netherlands,

Norwegian Research Council,

State Committee for Scientific Research, Poland, 2P03B06015, 2P03B03311 and SPUB/P03/178/98,

JNICT-Junta Nacional de Investigação Científica e Tecnológica, Portugal,

Vedecka grantova agentura MS SR, Slovakia, Nr. 95/5195/134,

Ministry of Science and Technology of the Republic of Slovenia,

CICYT, Spain, AEN96-1661 and AEN96-1681,

The Swedish Natural Science Research Council,

Particle Physics and Astronomy Research Council, UK,

Department of Energy, USA, DE-FG02-94ER40817.

## References

- [1] S.J. Brodsky and J.F. Gunion, Phys. Rev. Lett. 37 (1976) 402.
- [2] DELPHI Collab., P. Abreu et al., Eur. Phys. J. C4 (1998) 1.
- [3] DELPHI Collab., K. Hamacher, O. Klapp, P. Langefeld, M. Siebel et al., *Scaling Violations of Quark and Gluon Fragmentation Functions*, contributed paper 147 to the ICHEP'98 Conference, Vancouver, July 22-29, 1998.
- [4] Ya.I. Azimov, Yu.L. Dokshitzer, V.A. Khoze, and S.I. Troyan, Phys. Lett. 94B (1985) 147, Sov. J. Nucl. Phys. 43 (1986) 95.
- [5] V.A. Khoze, S. Lupia and W. Ochs, Eur. Phys. J. C5 (1998) 77.
- [6] DELPHI Collab., O. Passon, J. Drees and K. Hamacher et al., *Energy Dependence of Inclusive Spectra in  $e^+e^-$  Annihilations*, contributed paper 138 to the ICHEP'98 Conference, Vancouver, July 22-29, 1998.
- [7] K. Konishi, A. Ukawa, G. Veneziano, Phys. Lett. B78 (1978) 243;  
A.H. Mueller, Nucl. Phys. B241 (1984) 141;  
J.B. Gaffney, A.H. Mueller, Nucl. Phys. B250 (1985) 109;  
E.D. Malaza, B.R. Webber, Phys. Lett. B149 (1984) 501;  
E.D. Malaza, Zeit. Phys. C31 (1986) 143;  
I.M. Dremin and R. Hwa, Phys. Lett. B324 (1994) 477;  
I.M. Dremin and V.A. Nechitailo, Mod.Phys.Lett.A9 (1994) 1471.
- [8] DELPHI Collab., P. Abreu et al., Z.Phys.C70 (1996) 179-195.
- [9] for a compilation see: J. Fuster et al., Proc. of QCD 96, S. Narison ed., Nucl. Phys. B (Proc. suppl.) 54A (1997).
- [10] CLEO Collab., M.S. Alam et al., Phys. Rev. D56 (1997) 17-22.
- [11] OPAL Collab., G. Alexander et al., Phys.Lett. B388 (1996) 659-672.
- [12] ALEPH Collab., R. Barate et al. Z. Phys. C76 (1997) 191-199.
- [13] Yu.L. Dokshitzer, V.A. Khoze and S.I. Troyan, Sov. J. Nucl. Phys. 47 (1988) 881.
- [14] S. Marti i Garcia, Tesi Doctoral, Univ. de València (1995).
- [15] O. Klapp, Diplomarbeit, Bergische Univ. - GH Wuppertal, WUD 95-15 (1995);  
M. Siebel, Diplomarbeit, Bergische Univ. - GH Wuppertal, WUD 97-43 (1997).
- [16] DELPHI Collab., P. Aarnio et al., Nucl. Instrum. Meth. A303 (1991) 233-276;  
DELPHI Collab., P. Abreu et al., Nucl. Instrum. Meth. A378 (1996) 57-100,  
(Erratum-ibid.A396:281,1997).
- [17] S. Catani, Yu.L. Dokshitzer, M. Olsson, G. Turnock and B.R. Webber, Phys. Lett B 269 (1991) 432-438.
- [18] T. Sjöstrand, Comp. Phys. Comm. 39 (1986) 347.
- [19] DELPHI Collab., P. Abreu et al., Z. Phys. C 73 (1996) 11-59.
- [20] Yu. Dokshitzer, V.A. Khoze, A.H. Mueller and S.I. Troyan, *Basics of Perturbative QCD*, Editions Frontières, (1991).
- [21] B.R. Webber, Phys. Lett. 143B, (1984) 501.
- [22] R.K. Ellis, W.J. Stirling, and B.R. Webber, *QCD and Collider Physics*, Cambridge Univ. Press, (1996).
- [23] G. F. A. Marquis de l'Hôpital, *Analyse des infiniment petits pour l'intelligence des lignes courbes*, Paris 1692
- [24] G. Marchesini et al., Comp. Phys. Comm. 67 (1992) 465.
- [25] P. Eden, LU-TP-98-11, (1998) and hep-ph 9805228.
- [26] Yu.L. Dokshitzer, V.A. Khoze and S.I. Troyan, Int. J. Mod. Phys. A7 (1992) 1875, see also [29].
- [27] V.A. Khoze, private communication.

- [28] J.B. Gaffney and A.H. Mueller, Nucl. Phys. B250 (1985) 109, A.H. Mueller, Nucl. Phys. B241 (1984) 141.
- [29] V.A. Khoze and W. Ochs, Int. J. Mod. Phys. A12 (1997) 2949.
- [30] DELPHI Collab., P. Abreu et al.,  
*Charged particles from the Hadronic Decay of W Bosons and in  $e^+e^- \rightarrow q\bar{q}$  at 183 GeV*, contributed paper 287 to the ICHEP'98 Conference, Vancouver, July 22-29, 1998.
- [31] P. Abreu, Nucl. Phys. B (Proc. Suppl.) 71 (1999) 164
- [32] TASSO Collab., W. Braunschweig et al., Z. Phys. C45 (1989) 193;  
TPC Collab., Phys. Lett. 184B, 299;  
MARK-II Collab., Phys. Rev. Lett. 54, 2580;  
HRS Collab., Phys. Rev. D34, 3304;  
AMY Collab., Phys. Rev. D42, 737.
- [33] Yu.L. Dokshitzer and S.I. Troyan, Proc. of the XIX Winter School of the LNPI, Vol. 1, P. 144, Leningrad (1984), Ya. I. Azimov, Yu.L. Dokshitzer, V.A. Khoze and S.I. Troyan, Z. Phys. C 27 (1985) 65.
- [34] S. Moretti, L. Lonnblad and T. Sjöstrand, J.High Energy Phys. 8 (1998) 1.
- [35] I.M. Dremin and V.A. Nechitailo, Mod.Phys.Lett.A9 (1994) 1471.  
I.M. Dremin, JETP.Lett. 68 (1998) 559.
- [36] ALEPH Collab., R. Barate et al., Z. Phys. C76 (1997) 1;  
DELPHI Collab., P. Abreu et al., Phys. Lett. B414. (1997) 401-418;  
OPAL Collab., Z. Phys. C65 (1995) 367-377.
- [37] I.G. Knowles et al., in *Physics at LEP2*, CERN 96-01, Vol. 2, P. 111.
- [38] HEPDATA database, <http://cpt1.dur.ac.uk/HEPDATA>; see also M. R. Whalley, *HEPDATA - World Wide Web User Guide*, DPDG/96/01.